Mon. Not. R. Astron. Soc. **000**, 1–15 (2009) Printed 22 November 2007 (MN LATEX style file v2.2)

Population synthesis of binary pulsars.

S. Osłowski[1⋆†] and T. Bulik[1,2] and D. Gondek-Rosińska[3,2,4] and K. Belczyński[5,6]
[1] *Astronomical Observatory, University of Warsaw, Aleje Ujazdowskie 4, 00-478, Warsaw, Poland*
[2] *Nicolaus Copernicus Astronomical Centre, Bartycka 18, 00716 Warszawa, Poland*
[3] *Institute of Astronomy, University of Zielona Gòra, Lubuska 2, 65-265 Zielona Gòra, Poland*
[4] *LUTH, Observatoire de Paris, Universite Paris 7, Place Jules Janssen, 92195 Meudon Cedex, France*
[5] *New Mexico State University, Department of Astronomy, 1320 Frenger Mall, Las Cruces, NM 88003-8001, USA*
[6] *Los Alamos National Lab, PO Box 1663, MS 466, Los Alamos, NM 87545, USA*

Accepted . Received ; in original form

ABSTRACT
Using the StarTrack binary population synthesis code (Belczynski et al. 2008) we model the population of binary pulsars in the Galaxy. We include the detailed treatment of the spin evolution of each pulsar, due to such processes as spin-down, spin-up in the accretion events and magnetic field decay. We also model the spatial distribution of the binary pulsars due to their propagation in the Galactic gravitational potential. Newly born neutron stars are given natal kicks. This synthetic pulsar population is compared to the observed sample of binary pulsars taking into account the selection effects of detection in the radio band, to determine the best fit evolutionary parameters. With these parameters we determine the properties of the double neutron star binaries detectable in gravitational waves by the high frequency interferometer LIGO and VIRGO. In particular, we discuss the distributions of chirp masses and mass ratios in the radio and in the gravitational wave selected sample.

Key words: binaries: general – stars: neutron – stars: statistics.

1 INTRODUCTION

Double neutron stars (DNS) are remarkable objects in astrophysics and their studies uniquely contribute to a number of areas. The monitoring of PSR 1913+16 provided strong limits on the General Theory of Relativity (Hulse & Taylor 1975). The recent discovery of the first system with two observable pulsars J0737-3039 (Burgay et al. (2003) and Lyne et al. (2004)) has been a breakthrough in pulsar studies. The eclipses in this system provide insight in the physics of the magnetosphere (Lyutikov & Thompson 2005). The possibility of measurement of the moment of inertia of pulsar A in this system may lead to very strong constraints on the neutron star equation of state. DNSs are the only compact object binaries that we can study and deduce from their properties that there is a population of merging binaries - sources of gravitational waves for the LIGO and VIRGO observatories (Abramovici et al. (1992) and Bradaschia et al. (1991))

The origin of DNSs has been first worked out by Flannery & van den Heuvel (1975) in the context of the the Hulse Taylor pulsar PSR 1913+16. The birth rate and properties of DNSs were investigated by Piran (1992), and by Arzoumanian et al. (1999). Belczyński & Kalogera (2001) pointed out that there may exist a large population of ultra-compact DNS binaries formed with an additional common envelope stage, and not detectable in the radio. The existence of this population relies strongly on the result of the common envelope phase with a star on the Hertzsprung gap.

The investigation of pulsar evolution was first attempted by Gunn & Ostriker (1970) soon after the discovery of pulsars. Most papers concentrated on the modelling of the observed sample of pulsars with the inclusion of all selection effects and modeling of the pulsar evolutionary parameters such as initial distributions, magnetic field decay, evolution of inclination etc. (Large (1971), Taylor & Manchester (1977), Lyne et al. (1985), Stollman (1987), Emmering & Chevalier (1989), Bhattacharya et al. (1992), Hartman et al. (1997), Kalogera et al. (2001) Arzoumanian et al. (2002), Gonthier et al. (2002), Gonthier et al. (2004), Faucher-Giguère & Kaspi (2006)). These efforts were mostly concentrated on the classical pulsars and recently Story et al. (2007) have presented models of the population of recycled millisecond pulsars. However, they do not take into account the effects of binary evolution leading to formation of these objects but assume

⋆ E-mail: soslowski@astro.swin.edu.au
† Currently at Centre for Astrophysics and Supercomputing, Swinburne University of Technology, P.O. Box 218, Hawthorn, VIC 3122, Australia

initial injected distributions of magnetic fields and spin periods. For a review on binary pulsars see Lorimer (2008).

The evolution of binaries leading to formation of double compact objects has been investigated by many authors (Gnusareva & Lipunov 1985; Brandt & Podsiadlowski 1995; Jorgensen et al. 1995; Lipunov et al. 1995; Portegies Zwart & Yungelson 1998; Popov et al. 2000; Dewi et al. 2005; Bogomazov et al. 2005; Dewi et al. 2006; Kiel et al. 2008)

Here we will be using the Star Track binary population synthesis code which was presented and used in a series of papers by Belczynski and collaborators, see Belczynski et al. (2002), Belczynski et al. (2008) and references therein. The code has been used to investigate the possible binary progenitors of gamma ray bursts, and also to the rates and properties of binary gravitational wave sources (Bulik & Belczyński 2003; Bulik et al. 2004). Bulik et al. (2004) presented a calculation of the expected mass spectrum of merging compact object binaries including the double neutron stars. They hinted at a possibility of detecting a large number of non equal mass NS-NS binaries, and showed that they may not show up in the radio sample due to selection effects (Belczynski et al. 2002) .

In this paper we present the merger of two models: binary population synthesis and pulsar evolution models and compare them with the available data. In section 2 we present the model of the binary evolution and the pulsar evolution we use. Section 3 contains the results and comparison with the observations. Section 4 is devoted to comparison of the radio and gravitational wave selection effects, while Section 5 contains the conclusions.

1.1 Properties of known binary pulsars

There are currently 10 known pulsars in nine NS-NS binaries. In one case, both stars in the binary are visible as radio pulsars (J0737-3039). At Fig. 1 we present the spin period - spin period derivative diagram ($P-\dot{P}$) for this binaries. Most of the objects are concentrated in the millisecond pulsar region. However there are two noticeable outliers: J07373-3039B, the companion of the J07373-3039A in the binary pulsars system; and J1906-0746, a young pulsar with a likely neutron star companion. Detailed properties of those systems can be found in Tab. 1 (Stairs (2004),Faulkner et al. (2005) and Kasian (2008)). The binaries in Tab. 1 are ordered according to the merger time (time remaining to the coalescence). Three binaries at the bottom of the table have merger times much longer than 10 Gyr. We list the spin period and its derivative, the masses of the neutron star, as well as the present orbital parameters. The distribution of the orbital periods spreads over two orders of magnitude, with no clear evidence of clustering in these range, and the orbits of all systems are significantly eccentric. The masses of the seven objects with the merger times below 10 Gyrs are determined very well and are in the range between 1.25 and 1.44 $M_\odot$. The masses of the neutron star in the remaining three binaries are not so well constrained and may even lie outside this range.

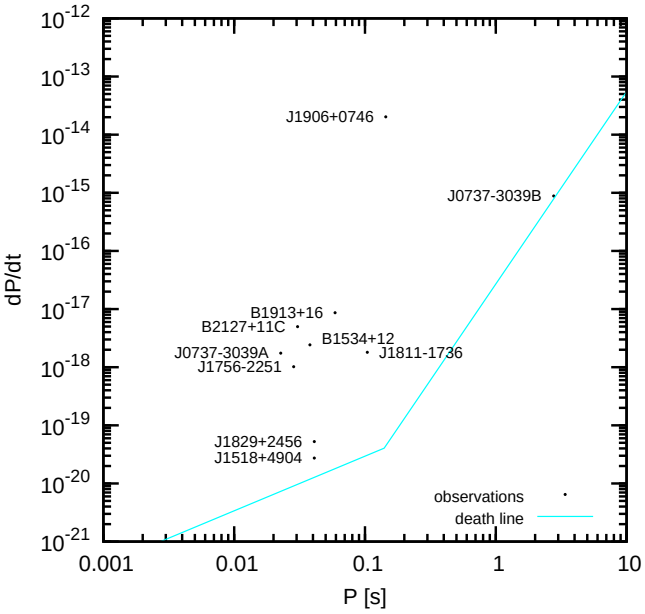

Figure 1. Observed binary pulsars on $P-\dot{P}$ diagram. Name of each pulsar is given next to it. We currently know about 10 pulsars in NS-NS binaries. In one case both are visible as radio pulsars (J0737-3039). The death lines are described in section 2.3.8.

1.2 Radio pulsars and population observable in gravitational waves

Due to the selection effects observed sample of NS-NS binaries might differ from the intrinsic population. There is also a possibility that the population observed in radio will have different properties that the one observed in gravitational waves. The most obvious selection effect in radio is drop of observed flux proportionally to distance squared from the observer to the pulsar. Our radio-telescopes have limited sensitivity so we will not see the weakest and/or farthest pulsars. The binary pulsar population observed in radio is restricted so far to our Galaxy.

In this paper we assume that all pulsars with observed flux below ~ 1 mJy at 400 MHz are not detectable in radio. We also try to incorporate in our calculations a second important selection effect directly connected with the fact that the pulsars considered are in binaries. According to Faulkner (2004), while searching pulsars with stack search and phase modulation methods it is difficult to detect radio emission from neutron stars which are in binaries with orbital period within range [0.3 h; 4 h]. In general it is due to the fact that signal-to-noise ratio drops drastically due to variation of pulsar period in during the observation. There are of course different methods of detecting radio pulsars which are sensitive for pulsars of such properties. Furthermore this orbital period range was calculated for a pulsar with the spin period $P = 9$ ms (Faulkner 2004), and it may vary as a function of P.

However, our aim is to see how this selection effect influences the observed properties of the population. Binaries detectable in gravitational waves will be those with relatively small orbital separation. Namely, we assume that binaries with coalescence time longer than 10^{10} years are not visible in gravitational waves. In both Bulik et al. (2004) and

Table 1. Properties of the observed pulsars in NS-NS binaries. The table contains names, spin period, spin period derivative, orbital period, mass of observed neutron star, mass of the companion, eccentricity of the orbit and time to merger. All given digits are significant. Errors, where given, are $1-\sigma$ errors.

Name	P $[ms]$	$\dot{P}$ $[ss^{-1}/10^{-18}]$	P_{orb} [h]	M_{obs} $[M_\odot]$	M_{cmp} $[M_\odot]$	e	τ_{mrg} $[Gyr]$
J0737-3039A	22.70	1.74	2.454	$1.337^{+0.005}_{-0.005}$	$1.250^{+0.005}_{-0.005}$	0.088	0.085
J0737-3039B	2773	8.8×10^2	2.454	$1.250^{+0.005}_{-0.005}$	$1.337^{+0.005}_{-0.005}$	0.088	0.085
B2127+11C	30.53	4.99	8.05	$1.35^{+0.04}_{-0.04}$	$1.36^{+0.04}_{-0.04}$	0.681	0.2
J1906+0746	144.07	2.028×10^4	3.98	$1.248^{+0.018}_{-0.018}$	$1.365^{+0.018}_{-0.018}$	0.085	0.3
B1913+16	59.03	8.63	7.752	$1.4408^{+0.0003}_{-0.0003}$	$1.3873^{+0.0003}_{-0.0003}$	0.617	0.3
J1756-2251	28.46	1.02	7.67	$1.40^{+0.02}_{-0.03}$	$1.18^{+0.02}_{-0.03}$	0.181	1.7
B1534+12	37.90	2.43	10.098	$1.3332^{+0.001}_{-0.001}$	$1.3452^{+0.001}_{-0.001}$	0.274	2.7
J1811-1736	104.182	0.091	451.20	$1.62^{+0.22}_{-0.55}$	$1.11^{+0.53}_{-0.15}$	0.828	>10
J1518+4904	40.935	0.02	207.216	$1.56^{+0.13}_{-0.45}$	$1.05^{+0.45}_{-0.11}$	0.249	>10
J1829+2456	41.0098	0.05	28.0	$1.14^{+0.28}_{-0.48}$	$1.36^{+0.50}_{-0.17}$	0.139	>10

Gondek-Rosińska et al. (2005b) the authors suggest that there will be differences between the two observed populations. In particular they reached the result that the mass ratio distributions will not be the same. The population modelling in those papers was quite crude. The binaries with lifetimes above the Hubble time were neglected, and it has been assumed that observability of pulsars is proportional to its lifetime. Such difference between the observed population in the radio in gravitational waves would be quite important as we need to know how the gravitational waves signal looks like to detect it. In order to know this signal we need the initial parameters for numerical relativity calculations. Until recently most calculations of coalescing neutron star binaries and black hole binaries assumed that mass ratio q is close to unity (e.g. Gondek-Rosińska et al. (2007), Buonanno et al. (2006)). In this paper we present carefully model the binary pulsar population with the updated stellar evolution code (Belczynski et al. 2008) combined with the detailed pulsar evolution model.

2 DESCRIPTION OF THE MODEL

2.1 StarTrack binary population synthesis code

In order to perform population synthesis of the binary pulsars we needed to know how the population of NS-NS binaries itself looks like. We used the *StarTrack* code for this purpose (Belczynski et al. 2008) . This code has been improved for many years now and is considered to be state-of-the-art with regard to our current understanding of stellar evolution. *StarTrack* has been extensively tested, calibrated and its results were compared with observations (e.g. Belczynski et al. (2002), Belczynski & Bulik (2002) or Belczynski et al. (2002)). At the base of this code are the analytic formulae describing evolution of single stars first developed by Hurley et al. (2000). The code follows sequence of evolutionary phases of stars starting at main sequence, passing through Hertzsprung gap, red giant branch or asymptotic giant branch. After the nuclear evolution of star ends it can form a compact object (white dwarf, neutron star or black hole). It can be also completely disrupted during supernova explosion leaving no remnant at all. StarTrack includes also the evolution of helium stars. If a star which first evolved ends up as a white dwarf or a neutron star then there is a chance for formation of a double neutron star system, provided that the binary is not disrupted during supernovae explosions. In the current version of StarTrack (Belczynski et al. 2008) in a standard model we assume bimodal distribution of the FeNi core masses in pre-supernova stars (Weaver & Weaver & Woosley (1993), Timmes et al. (1996)) stars with initial masses below $\sim 18-19$ $M_\odot$ burn carbon convectively forming cores of ~ 1.5 (NS of 1.3 $M_\odot$), while stars of higher mass burn carbon radiatively and the cores are more massive ~ 2 (NS of 1.8 $M_\odot$). The mass of the FeNi core does not depend sensitively on the initial star mass, but is a strong function of burning reactions within the pre-supernova star, and if similar reactions are encountered over a wide initial star mass range in which neutron stars are formed (e.g. 8-18 $M_\odot$) then the majority of neutron stars are expected to have similar masses. The previously employed neutron star mass calculation was based on stellar evolutionary modeling that was suggestive of increase of final FeNi core mass with initial star mass (e.g.. Weaver & Woosley (1993); or see Table 4.4 of Vanbeveren et al. (1998)); that naturally resulted in a wide neutron star mass spectrum.

Some poorly known details of stellar evolution are parametrized in the *StarTrack* code. Fortunately most of them do not have significant impact on the results relevant for this work. The various models of binary code used in this paper are described in section 2.2.1.

2.2 Evolution of the binaries

We consider three variants of the binary population synthesis models. They are described in detail below.

2.2.1 Model A - standard

This model is described in detail in Belczynski et al. (2002) and updated in Belczynski et al. (2008). Here we present only its most important features. Initial mass of heavier (at the time of formation) star is drawn from power law $\sim M^{-2.7}$ (Scalo 1986). Mass of the second star is a fraction of it randomly chosen from a flat distribution (Kuiper 1935), the initial orbital separation is flat in logarithm, and we draw

the initial eccentricity from a flat distribution. The code calculates the carbon-oxygen core mass which will form a compact object using formulae from already mentioned work by Hurley et al. (2000). This mass has impact on the mass of newly formed neutron star due to its influence on a mass of Fe-Ni core as described in Woosley (1986), Fryer et al. (1999) and Timmes et al. (1996) .

$$M_{NS} = \begin{cases} M_{FeNi}, & M_{CO} \leqslant 5M_{\odot} \\ M, & M_{CO} \geqslant 7.6M_{\odot} \\ M_{FeNi} + f_b(M - M_{FeNi}), & otherwise \end{cases},$$

where f_b is a fall-back factor (describing what fraction of the stellar envelope falls back), M_{FeNi} is Fe-Ni core mass, M_{CO} is CO core mass and M is pre-SN mass of the star. Orbital parameters are affected by tidal interactions, mass loss due to stellar winds, mass transfers, and gravitational waves emission. We parametrize the fraction of mass ($f_a = 0.5$) taking part in stable mass transfer that is accreted on companion and the rest is lost from the binary. Unstable mass transfer in *StarTrack* (common envelope - CE) are treated with the formalism proposed by Webbink (1984) and de Kool (1990). In this model we assume $\alpha_{CE} \times \lambda = 1.0$. Neutron star can accrete some mass during the common envelope phase. The amount of this mass is drawn from a range $[0.05M_{\odot}, 0.10M_{\odot}]$ with flat distribution. Supernova explosions are treated with details: the explosion occurs at a random place in the orbit, we take into account natal kicks drawn from Hobbs et al. (2005) distribution, and calculate the orbit and center of mass velocity after the explosion. This model is described in detail in Belczynski et al. (2008) and is referred further as the model A, the standard model. The following two section describe two other models that differ from A.

2.2.2 Model H

The common envelope phase is treated differently in this case so that a neutron stars accrete more matter. It has crucial impact both on binary evolution (changes in orbital separation) and on properties of the pulsar which formed first. In this model we assume Bondi-Hoyle accretion (Bondi & Hoyle 1944) with a hypercritical accretion rate (Brown et al. 2000). The amount of accreted mass is roughly 10 bigger than in the standard model A. This amount depends mostly on mass ratio in the binary prior to the common envelope q_0. Final mass is calculated using formula (Bethe & Brown 1998):

$$M_B = \left(q_0 + 0.7q_0^2\right) M_A$$

where M_B is the mass of the acceptor after the transfer and M_A is the mass of the donor before the transfer.

2.2.3 Model S

In this model we assume a different initial mass function of newly formed neutron stars. It assumes very simplified linear relation between M_{NS} and the mass of the iron core M_{core} from which it is formed:

$$M_{NS} = 0.35 \times M_{core} + 0.596M_{\odot}.$$

The values of parameters are such that we have neutron stars with masses from $1.1M_{\odot}$ (forming from a star with mass $8.275M_{\odot}$ on a zero age main sequence) to $2.5M_{\odot}$ (forming from a star with mass $20.88M_{\odot}$ on a zero age main sequence). The purpose of this model is to check the influence of this poorly known relation on double neutron star mass distributions.

2.3 Pulsar evolution model

In this section we describe the modelling of processes important in evolution of pulsars in binaries. At the very beginning we assign each neutron star a set of initial parameters such as spin period, magnetic field and moment of inertia. After that we start evolving each pulsar. First of all we need to know how its rotation behaves in time. We assume dipole model for the magnetic field. We also present how mass transfers influence neutron stars (e.g. recycling). During accretion neutron stars are visible in X-rays but in this paper we neglect that as this periods are short compared to radio activity periods. We finish the evolution of a binary pulsar either at the time of coalescence due to gravitational wave emission or when it reaches the age of 10 Gyr. During the evolution we note the radio loud periods in the history of the binary, and also the periods it is visible in the radio from Earth.

2.3.1 Initial parameters

Each neutron star is evolved as a pulsar right after it is formed. Its initial magnetic field B_0 is drawn from range $[10^{11}\mathrm{G}, 10^{13}\mathrm{G}]$ with a flat logarithmic distribution (Faucher-Giguère & Kaspi 2006). Each pulsar is assigned an initial spin period $P_{ini} = 10$ ms (Cordes et al. 2004). We assume that each pulsar has the same P_{ini} because even if some pulsars are born with longer or shorter periods then it does not change the overall properties of the population. It is so due to the fact that rotation of a young pulsar evolves very quickly so that a young neutron star on a short time scale moves on the $P - \dot{P}$ diagram towards higher spin periods.. All the neutron stars are of equal radius $R = 10$ km and a moment of inertia $I = 10^{45}$ g $\times$ cm^2. We consider the spin-down only to to the electromagnetic radiation so the braking index n=3. The initial rotation frequency time derivative is:

$$\dot{\Omega} = -\frac{B^2 R^6 \sin^2 \alpha}{6c^3 I}\,, \tag{1}$$

where α is the angle between rotation and magnetic field axis, B is the magnetic field, R is the neutron star radius, c is the speed of light and I is the moment of inertia of the neutron star. We assume $\alpha = 90°$. for each pulsar. The magnetic field value and the angle α are degenerate so we are not losing anything in making this assumption. The observations show that the breaking indexes of pulsars are in the range $\approx 2.5 - 3.5$ (Manchester et al. 2005). At every point of evolution the magnetic field is given by

$$B = 3.2 \times 10^{19} \sqrt{P\dot{P}}\ \mathrm{Gauss}\,. \tag{2}$$

2.3.2 Evolution of the magnetic field

There are no direct interactions between companions after formation of both neutron stars (except for coalescence and

contact of magneto-spheres). At this stage the spin period and its evolution do not depend in any way on companion's properties. If this statement is true for a given numerical step then we call it a standard step. We can have such steps also in the time between formation of first and second neutron star if there are no mass transfers ongoing. In the standard step we calculate current spin period and its derivative according to equation 1. In addition we assume magnetic field of a pulsar is decaying exponentially in time:

$$B = (B_0 - B_{min}) \cdot \exp\left(-\frac{t}{\tau_d}\right) + B_{min} \ , \tag{3}$$

where τ_d is the magnetic field decay time scale. The decay of the magnetic field is controversial with some analyses showing that it proceeds on a timescale of $2 - 5$Myrs (Gonthier et al. 2002, 2004), while other (Faucher-Giguère & Kaspi 2006) arguing that it may be an artifact of the assumed luminosity law. We include it as in general there seems to be some torque decay in pulsar evolution (Faucher-Giguère & Kaspi 2006). The pulsar which formed earlier can be an exception as we assume that after it accretes any amount of mass its field ceases to decay. We also assume that there is a lower limit for the strength of magnetic field $B_{min} = 10^8$ G., i.e. that the magnetic field decay ceases once the field reaches this value.

2.3.3 Roche lobe overflow

Before the second supernova explosion occurs, the companion of an already formed pulsar continues its stellar nuclear evolution. It can fill its Roche lobe in this period. If that is the case then there is mass transfer from the companion and the system becomes an X-ray binary. Some mass is lost from the system and some is accreted onto the neutron star. Besides increase of the mass of the neutron star mass, the mass transfer results in three effects:
(I) we assume that the magnetic field decays, and we model the magnetic field change as:

$$B = (B_0 - B_{min}) \cdot \exp\left(-\frac{dM}{\Delta M_d}\right) + B_{min} \ , \tag{4}$$

where dM is the accreted mass and ΔM_d is magnetic field decay mass scale , and B_{min} is the minimal magnetic field of a neutron star. After the mass accretion induced decay the field stops to decrease in time, i.e. it is fixed at the final level unless another mass transfer happens. In the latter case field decays in the same way as in the first event. The lower limit for the magnetic field also applies $B_{min} = 10^8$ G.
(II) the pulsar in the accretion phase is not emitting in the radio. This is because the magnetosphere is filled by the accreted gas, and the particle acceleration is not effective. The pulsar is visible in the X-ray band but in this work we do not model this phase.
(III) the spin period of a pulsar is affected. Due to angular momentum transfer the neutron star tends to corotate with the accreted matter at the Alfven radius:

$$R_A = \left(\frac{8R^{12}B^4}{M\dot{M}^2G}\right)^{\frac{1}{7}} \ .$$

The accretion rate $\dot{M}$ is calculated within the *StarTrack* code by considering the detailed evolution of the companion (Belczynski et al. 2008). The orbital velocity at Alfven radius equals:

$$\Omega_A = \sqrt{\frac{GM}{R_A^3}} \ .$$

If the amount of matter is sufficient, namely $dM > 0.1M_\odot$, then we assume that such corotation is attained and the pulsar is fully spun up. Note that if the matter at Alfven radius has angular velocity smaller than this of the neutron star, it can spin down the neutron star. In such cases the propeller effect might take place (see 2.3.6).

2.3.4 Partial spin-up

If the accreted mass is smaller than $0.1M_\odot$ then the pulsar can be spun-up to a smaller angular velocity. We assume that the amount angular is momentum transferred ΔJ is proportional to the accreted mass:

$$\Delta J \propto \frac{\Delta M}{0.1M_\odot} \ ,$$

This leads to a linear relation between the amount of accreted mass and the final angular velocity of the pulsar:

$$\Omega_f = \Omega_0 + (\Omega_A - \Omega_0)\frac{\Delta M}{0.1M_\odot} \ ,$$

where Ω_f is the final angular velocity, Ω_A is the angular velocity at the Alfven radius and Ω_0 is the initial angular velocity before recycling.

2.3.5 Common envelope

Formation of double neutron stars involves quite frequently an unstable mass transfer, i.e. a common envelope phase. During the common envelope phase the binary orbit is tightened, and a significant amount of matter from the companion is expelled. At the same time some matter is accreted onto the neutron star, see section 2.2.1 and references therein. In the *StarTrack* code the common envelope is treated following the (Webbink 1984) formalism and it is assumed that the amount of matter accreted by the neutron star lies in range $[0.05M_\odot, 0.10M_\odot]$ and is drawn from it with a flat distribution, which corresponds to highly super Eddington accretion rate. At this stage the angular momentum transfer is chaotic (Benensohn et al. 1997), and we assume that the spin of a neutron star is not affected on the average by accretion during this phase, i.e. the spin period of the pulsar is the same as before the common envelope. However, the accreted matter quenches the magnetic field of the neutron star, according to equation (4). Thus, a system after a common envelope phase has a tightened orbit, and the pulsar is more massive with decreased magnetic field yet its spin frequency is unchanged.

2.3.6 The propeller effect

Here we consider the case of a pulsar rotating with greater velocity than matter orbiting at the Alfven radius. Illarionov & Sunyaev (1975) suggested that in this case the propeller effect takes place: accretion onto neutron star is inhibited because of centrifugal force at the Alfven radius. This hypothesis is supported by the X-ray observations (Cui 1997).

In section 2.3.3 we describe how the accretion can spin up or down the neutron star. In models which include the propeller effect, we do not allow for the spin-down by accretion, however, we allow for the magnetic field decay and with no influence on the spin rate of the neutron star.

In the models where we neglect the propeller effect a neutron star can both be spun down or up. The outcome depends on the value of the magnetic field and on the accretion rate.

2.3.7 Evolution of the orbit

Some of the binaries are tight enough to be strongly influenced by gravitational waves emission. We calculate the orbit evolution due to emission of gravitational waves in first Post-Newtonian approximation. The time derivatives of the eccentricity and the semi-major axis are (Peters 1964):

$$\frac{da}{dt} = -\frac{64}{5}\frac{G^3(M_1+M_2)^2}{c^5 a^3(1-e^2)^{\frac{7}{2}}}\left[1+e^2\left(\frac{73}{24}+\frac{37}{96}e^2\right)\right]$$

$$\frac{de}{dt} = -\frac{304}{5}e\frac{G^3(M_1+M_2)^2}{c^5 a^4(1-e^2)^{\frac{5}{2}}}\left(1+\frac{121}{304}e^2\right)$$

Orbit evolution is taken into account for the entire time the binary is evolved, namely for 10 Gyr or until coalescence. The pulsars can be radio loud until the moment when the semi-major axis of system is smaller than the sum of light cylinder radii:

$$a < \frac{c}{2}\left(\frac{1}{\Omega_1}+\frac{1}{\Omega_2}\right),$$

where a is the semi-major axis, c is the speed of light, Ω_1 and Ω_2 are angular velocities of first and second pulsar respectively. The contact of magneto-spheres in practice does always happen in the same numerical step as the coalescence.

2.3.8 Radio luminosity

In order to check the influence of selection effects and to compare populations visible in gravitational waves and in radio we need to know the radio luminosity of all the pulsars. We use a Narayan & Ostriker (1990) model fitted to the observations:

$$\log_{10} L = \frac{1}{3}\log_{10}\left(\frac{\dot{P}_{-15}}{P^3}\right) + 1.635,$$

where $P_{-15} = \frac{\dot{P}}{10^{-15}}$. This luminosity is given in units of $mJy \times kpc^2$ for observations at 400 MHz.

The pulsars cease to emit in the radio once they cross the death lines. After crossing this lines on this diagram the pulsar's emission mechanism fails as electron-positron pairs can no longer be created in the magnetic field. We take two death lines into account (Rudak & Ritter 1994). In this work we assume that all the pulsars cease their emission after crossing the death lines defined by:

$$\log_{10}\dot{P} = 3.29 \times \log_{10} P - 16.55\ ,$$

$$\log_{10}\dot{P} = 0.92 \times \log_{10} P - 18.65\ .$$

These relations are rather empirical and there are cases when a pulsar is found beyond these death lines (Young et al. 1999), yet they describe the cutoffs on the P-$\dot{P}$ diagrams quite well.

2.3.9 Numerical step size

In order to choose the length of the numerical step size during the evolution of a DNS we calculate a number of time derivatives describing the rate of change of pulsar properties. The step is chosen in such a way to satisfy the following conditions: (i) the pulsar period changes by less than 1% (ii) the semi-major axis of the orbit changes by less than a 1%, (iii) the step is limited by the beginning of the next mass transfer episode, (iv) the time step is shorter than 1 Gyr. The last condition was introduced to follow the evolution of recycled millisecond pulsars with weak field on large orbits.

2.3.10 Free parameters

We list the parameters describing the evolution of pulsars in Table 2. We consider several models of pulsar evolution and we list them along with the values of the evolutionary parameters in Table 3. We choose the following notation to denote each model: the first letter in the name of model refers to the stellar evolution model in the *StarTrack* code; the letter P means that the model incorporates the propeller effect. The letter F implies that no partial spin-up is possible in given model, all the pulsars are recycled to the orbital velocity at Alfven radius regardless of the amount of accreted matter; the letters D and T are followed by numbers referring to the magnetic field decay - respectively mass(ΔM_d) and time (τ_d) scales.

2.3.11 Motion in the Galaxy

In order to obtain the observed radio fluxes of the pulsars we need to model their motion in the Milky Way. Therefore we consider a simple model of the Galaxy consisting of the following three components: bulge, disk, and halo. The bulge and disk potential are described by the Miyamoto & Nagai (1975) type potential (Paczynski 1990; Bulik et al. 1999):

$$\Phi(r,z) = \frac{GM}{\sqrt{R^2+(a+\sqrt{z^2+b^2})^2}}\,,$$

where M is the mass of a given component, $R=\sqrt{x^2+y^2}$, and a, b are the parameters. The halo is described by the density distribution $\rho = \rho_c[1+(r/r_c)^2]^{-1}$ with a cutoff at $r_{cut} = 100\,\mathrm{kpc}$ above which the halo density is zero. The corresponding potential for $r < r_{cut}$ is

$$\Phi(r) = -\frac{GM_h}{r_c}\left[\frac{1}{2}\ln\left(1+\frac{r^2}{r_c^2}\right)+\frac{r_c}{r}\arctan\left(\frac{r}{r_c}\right)\right]$$

We use the following values of the parameters (Blaes & Rajagopal 1991) describing the bulge (index 1) and disk (index 2) potential: $a_1 = 0\,\mathrm{kpc}$, $b_1 = 0.277\,\mathrm{kpc}$, $a_2 = 4.2\,\mathrm{kpc}$, $b_2 = 0.198\,\mathrm{kpc}$, $M_1 = 1.12\times10^{10}\,M_\odot$, $M_2 = 8.78\times10^{10}\,M_\odot$, while for the halo potential we use $M_h = 5.0\times10^{10}\,M_\odot$, and $r_c = 6.0\,\mathrm{kpc}$. The distribution of stars in the disk is assumed to be that of a young disc

Table 2. Free parameters in the evolution model

Parameter	Description	Default value
τ_d	Time scale of field decay	5 Myr
ΔM_d	Mass scale of field decay	0.025 $M_\odot$
B_0	Initial magnetic field	$[10^{11}$ G, 10^{13} G]
B_{min}	Minimal magnetic field	10^8 G
I	Moment of inertia	10^{45} g $\times$ cm^2
R	Pulsar radius	10 km
α	Angle between rotation and magnetic axis	90°
–	Mass limit for full spin-up	0.1 M$_\odot$

(Paczynski 1990). The radial and vertical distributions are independent i.e. the distributions factor out:

$$P(R,z) \propto R(R)dR\,p(z)dz\,,$$

where the radial distribution is $p(R) \propto \exp(-R/R_{exp})$, and $R_{exp} = 4.5\,$kpc, and we introduce an upper cutoff at $R_{max} = 20\,$kpc. The vertical distribution is exponential $p(z) \propto \exp(-z/75\mathrm{pc})$. After distributing the binaries with the given densities, we evolve them in time. We use the leapfrog method in KDK scheme with a constant (10^5 years) time step. This approach is fully symplectic.

2.4 Detection in the radio band

We consider radio population to be composed of pulsars with non-zero radio luminosity. The radio luminosity of each pulsar is calculated at each time step. The radio luminosity of a pulsar drops to zero during mass transfers and after crossing the death lines. We define the radio population with selection effects as all objects with the fluxes at Earth above $1mJy$. Additionally the BNS with the orbital period between $0.3h$ and $4h$ may have decreased detectability (Faulkner 2004). We consider a population with and without such objects and we will discuss the differences (see 1.2). We neglect the fact that radio beams can have a limited width and the dispersion by electron gas in the Galaxy.

2.5 Detection in gravitational waves

The gravitational wave detectors such as LIGO: (Flanagan & Hughes 1998) and VIRGO (Kulczycki et al. 2006) are currently working and in principle can detect neutron star coalescence as far as 18 Mpc. The signal to noise ratio from the inspiral phase of two compact objects is given by

$$\frac{S}{N} \sim M_{chirp}^{\frac{5}{6}} \times \frac{1}{D}\,,$$

where D is a distance from the observer and chirp mass $M_{chirp} = (M_1 M_2)^{0.6}\,(M_1+M_2)^{-0.2}$, where M_1 and M_2 are masses of first and second star in the system respectively. We define the DNS population observable in gravitational waves as these with the merger time below the Hubble time and weight all their observable quantities with the volume in which they are observable, i.e.

$$V \sim M_{chirp}^{\frac{5}{2}}\,.$$

Thus the gravitational wave population is the population residing in multiple galaxies and we assume that the populations in these galaxies resembles the one in the Galaxy.

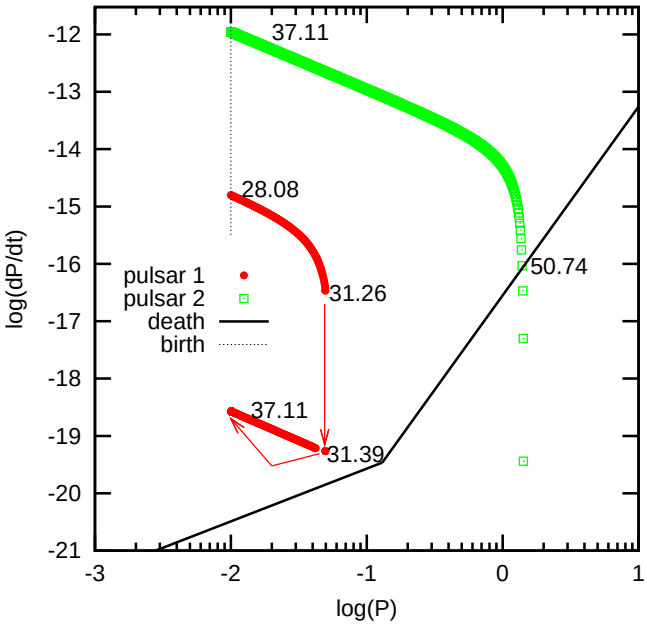

Figure 2. An example of a neutron star binary evolution on the $P-\dot{P}$ diagram. The dotted line corresponds to the birth line, where all neutron star are formed in our model. The solid lines represent the death lines. The numbers correspond to characteristic ages in Myrs and are explained in in the text (3.1). Arrows show how the mass transfer affects the first pulsar.

We neglect the possible detection of the gravitational waves in the merger and ringdown phases of the coalescence.

3 RESULTS

3.1 Example of a binary evolution

In subsection 2.3 we described our phenomenological model of pulsar evolution. In Fig. 2 we present an example of an evolutionary path leading to the formation of a double neutron star. The example is based on the model AF.

The pulsars are born with the rotational period $P_{ini} =$ 10 ms at the line of birth (the dotted line on Fig. 2). The initial value of the magnetic field ,which determines the spin period derivative, is drawn from a flat distribution as described in section 2.3. The binary starts on zero age main sequence at $t = 0$. The first pulsar is born after 28.08 Myrs. The system consists of a pulsar and a massive rejuvenated companion. The neutron star evolves in the $P-\dot{P}$ plane along the line of constant magnetic field. At t=31.26 Myrs

Table 3. Models of pulsar evolution

Model	τ_d	ΔM_d	propeller	spin-up	*StarTrack* model
A	5	0.025	no	partial possible	A
AF	5	0.025	no	only full	A
APD05	5	0.05	yes	partial possible	A
AP	5	0.025	yes	partial possible	A
APF	5	0.025	yes	only full	A
APT20	20	0.025	yes	partial possible	A
HP	5	0.025	yes	partial possible	H
SP	5	0.025	yes	partial possible	S

the nuclear evolution of the companion plunges the system into the common envelope phase. The magnetic field of the pulsar is quenched and it falls close to the death line. The companion loses the envelope and becomes a helium star while the neutron star reappears in radio. It barely evolves until $t = 37.11$ Myrs when the second mass transfer occurs, this time it is a stable Roche lobe overflow. The system becomes an X-ray binary and the neutron star is recycled to a period $\approx 0.01s$. The amount of accreted matter is very small ($\sim 10^{-5} M_\odot$) but in this model we allow for full recycling anyway. In other models we limit the accretion rate to the Eddington limit and consequently the recycling is weaker. Soon after this mass transfer the second pulsar is born, and for the following 23 Myrs the binary contains two radio loud pulsars. At around t=50.74 Myrs the second born pulsar falls below the death line. At this stage the system contains the recycled pulsar which slowly evolves to the death line. It does not reach it throughout the whole simulation, which ends after 10 Gyrs have passed. Some of the pulsars in our simulations manage to pass the death line before coalescence. This binary is relatively wide, so it does not coalesce within that time.

3.2 Standard model

In order to analyse the properties of the population of binary pulsars we have to take into account the selection effects. We define two types of selection effects that leads to differences between the intrinsic and the observed population. The first is the simple effects connected with the fact that any radio survey has limiting flux. We select the radio population as all pulsars with the observed flux on Earth $F > 1$mJy. Additionally, it has been noted that binaries with the orbital period between 0.3 and 4h are difficult to detect (Faulkner, 2004) so we also remove these systems from the observed population unless otherwise noted.

3.2.1 Population on $P - \dot{P}$

We start with the analysis of the population of binary pulsars on the $P-\dot{P}$ diagram. To obtain the present observable population of binary neutron stars we assume that star formation rate in the galaxy is constant. We place them in the Galaxy according to the model described in section 2.3.11, and we propagate them in the Galactic potential taking into account the additional kick velocities that the binary receives at birth of the two pulsars. We then look for the observable population taking into account the selection effects described above. The density of the objects in the $P-\dot{P}$ plane is found by summing the times that each pulsar spends in a given cell on the $\log P - \log \dot{P}$ plane, i.e. the density in the in a given cell on $P - \dot{P}$ is :

$$f_{ij} = \frac{F_{ij}}{F} \frac{1}{\Delta \log P \Delta \log \dot{P}} , \quad (5)$$

where $\Delta \log P = 0.08$ and $\Delta \log \dot{P} = 0.18$ denote bin width of spin period and its derivative respectively, $F = \sum_{i,j=1}^{50} F_{ij}$ and

$$F_{ij} = \sum_{p=1}^{N_{ij}} t_{ij}^p,$$

where N_{ij} is a count of simulated pulsars with P contained in the i-th and $\dot{P}$ in j-th bin and t_{ij}^p is a time p-th pulsar spends in these bins. Range of $\log_{10} P$ from -3 to 1 as well as $\log_{10} \dot{P}$ range from -21 to -12 were divided into 50 bins.

The density of the population in the $P-\dot{P}$ plane (shown on Fig. 3 and 4) is determined by the properties of the two component of the population: the first born, possibly recycled pulsar and in a much smaller degree by the second born pulsar. The details of the binary evolution and recycling are influencing strongly the region where we expect the recycled pulsars. For the models where we allow for the full spin-up (AF, APF) the population of millisecond pulsars extends to period below 20ms. Another model where there are many pulsars in this region is model HP, where we allow for very strong accretion and therefore recycling is always full. In model HP most pulsars end up in the small region with the pulsar period of approx 1-2ms, and period derivative of $\approx 10^{-21}$. In the remaining models the mass transfer leads to decrease of the field in the CE phase, but at the same time the period is not changed by much. Inclusion of the propeller effect (models denoted by P) limits the amount of accreted matter and thus may limits the field decay. This decreases slightly the density of pulsars with the lowest values of $\dot{P}$, see e.g. model A vs model AP. The time scale of the spontaneous decay of magnetic field does not influence the overall shape of the distribution in the $P - \dot{P}$ diagram see model AP and APT20. Finally, the magnetic field mass decay scale influences the values of the magnetic fields of the recycled pulsars and hence the distribution of their period derivatives $\dot{P}$, see model APD05 with the $\Delta M_d = 0.05\, M_\odot$ and AP with $\Delta M_d = 0.025\, M_\odot$. If the value of ΔM_d is large than the magnetic field of pulsar does not decay fast and they end up as millisecond recycled pulsars with a little stronger magnetic field in the region between 10^{-19} and 10^{-17}, while for the small value of ΔM_d the final magnetic

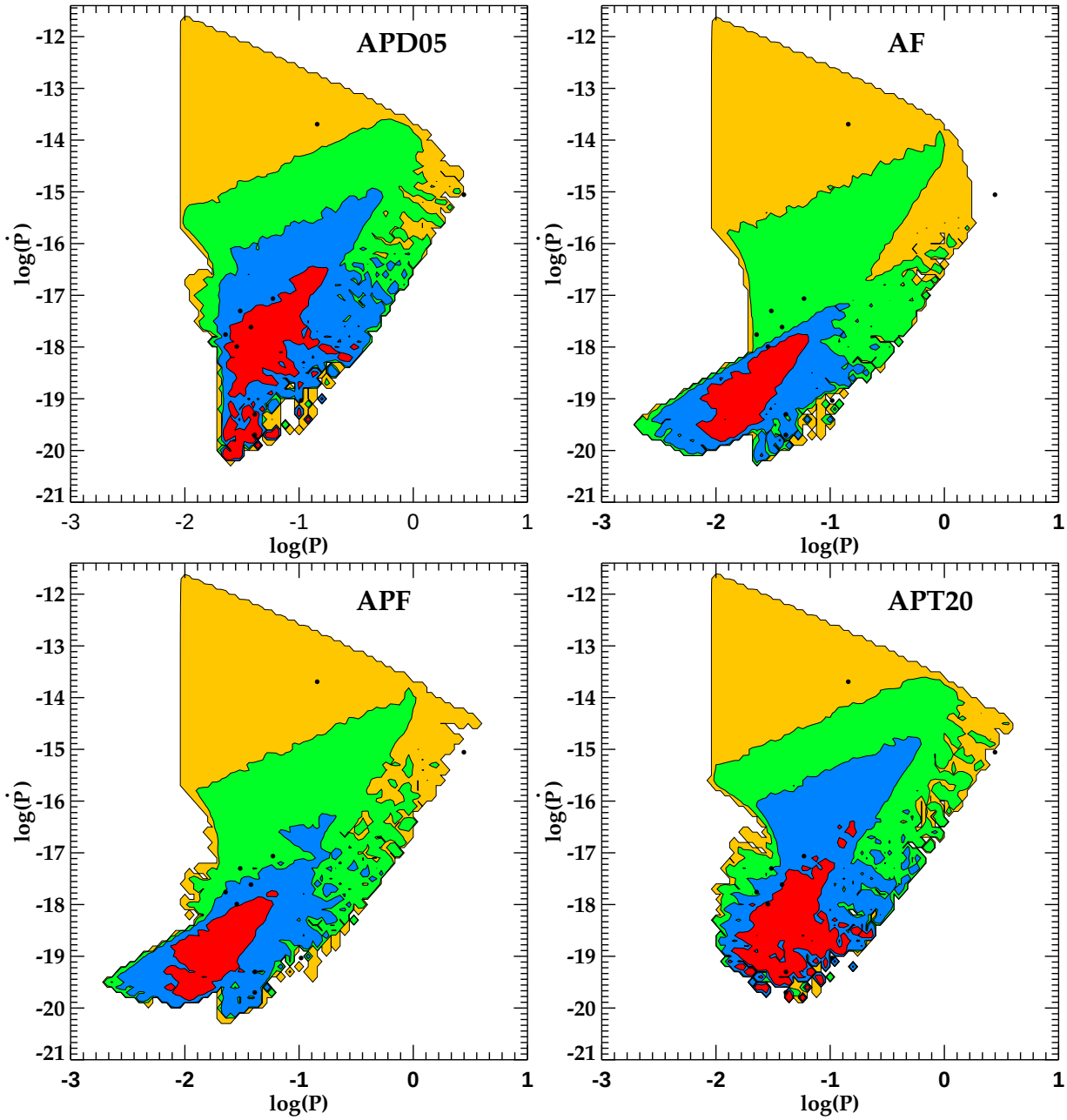

Figure 3. Probability density on $P - \dot{P}$ diagram within models APD05,AF,APF, and APT20. The levels correspond to contours containing 68, 95, and 99 percent of the objects. The outer contour delimits the region containing all the objects in the simulation. Black dots correspond to observations.

field of pulsars are lower and they populate the region below 10^{-18} - see model AP.

3.3 Comparison with observations

In order to quantify which model of the distribution in the $P - \dot{P}$ best describes the data we calculate the likelihood of each model given the data from Table 1. We define the likelihood as :

$$\mathcal{L} = \prod_{k}^{K} f(P_k, \dot{P}_k),$$

where $\mathcal{L}$ is the likelihood, P_k and $\dot{P}_k$ are period and its derivative values for a k-th observed pulsar (see Tab. 1) and f is the probability density defined by equation 5 in section 3.2.1. We use two sets of data to calculate the likelihood: (Comparison 1) the standard model, where we take into account the flux selection effect as well as rejection of pulsars with the orbital periods between 0.3 and 4h is compared with the data set with J0737-3039 A and B excluded as its orbital period lies in this range; (Comparison 2) the extended model where we do not reject the pulsars with the orbital periods between 0.3 and 4h is compared to the full data set of Table 1, and (Comparison 3) with the data set where we exclude J0737-3039B. We present the results in Table 4.

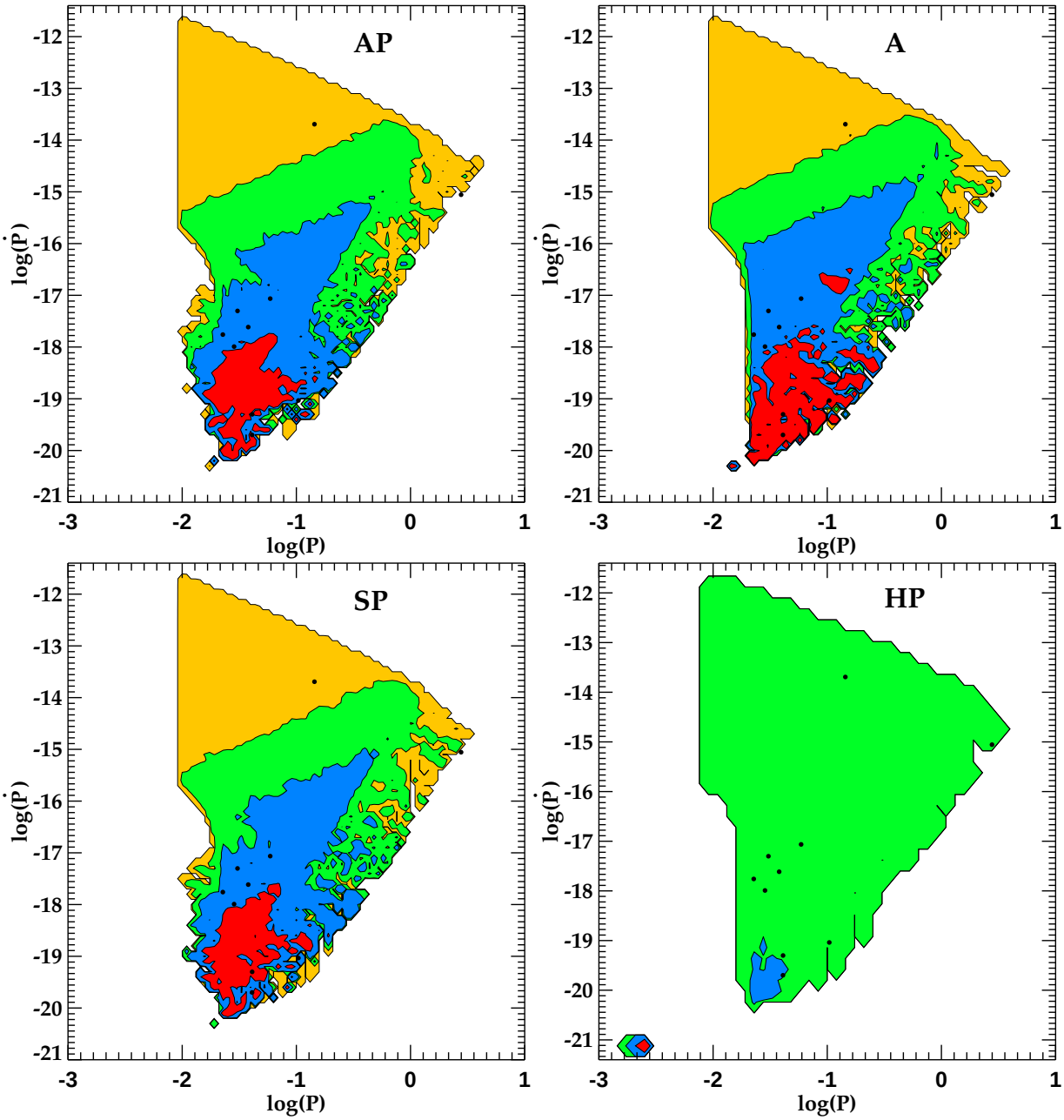

Figure 4. Same as Figure 3, for the models AP,A, SP, and HP. The yellow contour for HP model overlaps with the green one.

In all three comparisons in Table 3.3 the model APD05 best fits the data. This is a model with the propeller effect taken into account and with increased mass scale for the magnetic field decay. The models with the standard value lead to too small magnetic field of the synthetic sample. Increasing the magnetic field mass decay scale ΔM_d leads to smaller decay of the field. and therefore better agreement with the data. Also the models with full recycling are very far from the observations since they predict the population of pulsars in binaries with spin periods below 20ms.

4 EXPECTED MASSES OF NEUTRON STARS OBSERVED IN GRAVITATIONAL WAVES AND IN THE RADIO

In Bulik et al. (2004) the authors have calculated the expected masses of neutron stars observed in gravitational waves using the StarTrack population synthesis code (Belczyński et al. 2002 for detailed description). The assumed value for the minimum mass and maximum mass of a neutron star was 1.2 $M_\odot$ and 3.0 $M_\odot$ respectively. They have verified the results taking the maximum mass to be 2 $M_\odot$ and 2.5 $M_\odot$ (Gondek-Rosińska et al. 2005a). They have shown that the distributions of mass ratio q (defined as the ratio of less to more massive component) of neutron star binaries observed in gravitational waves, have two peaks:

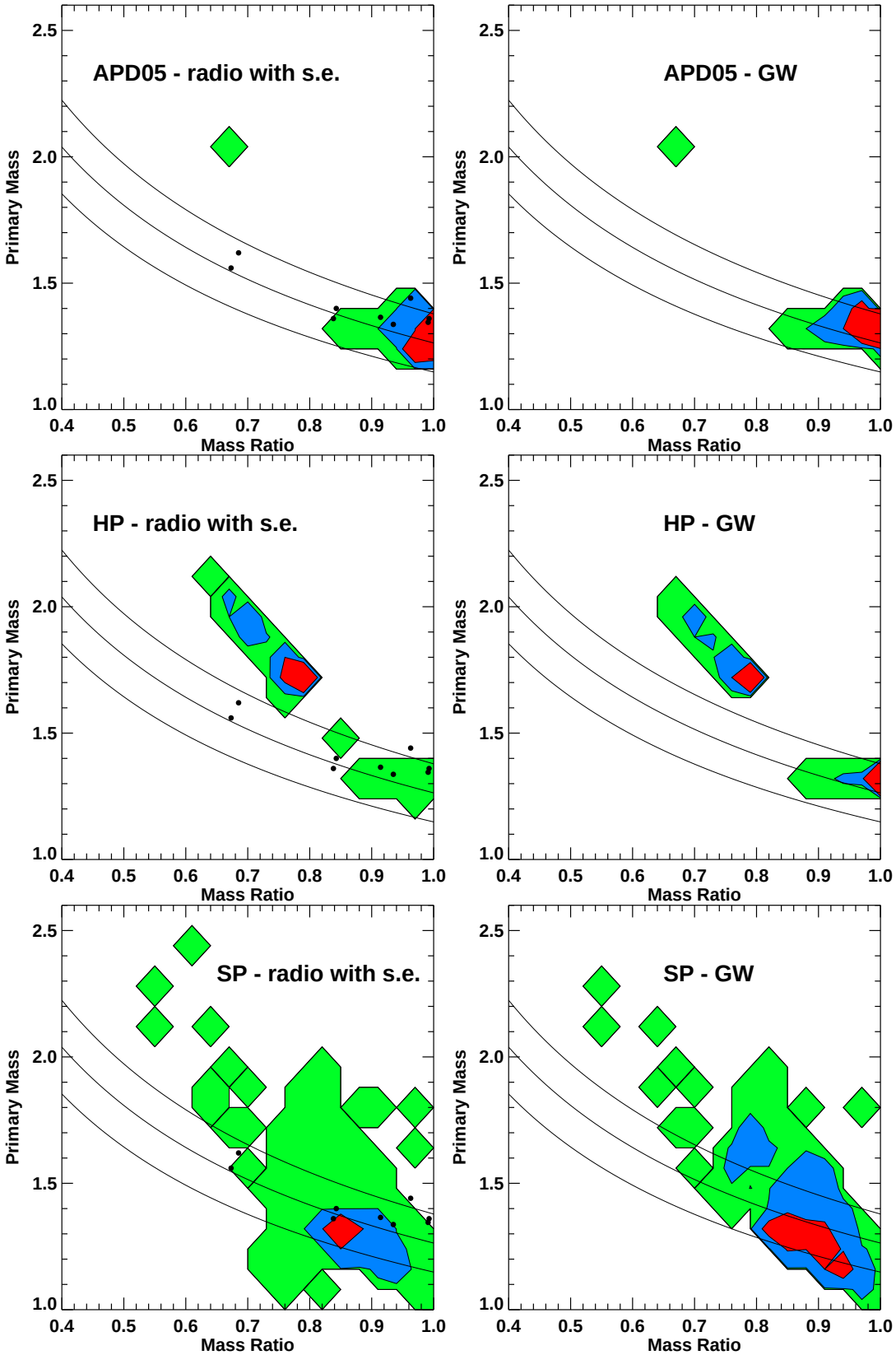

Figure 5. Distribution of masses (in $M_\odot$) and mass ratios observed for the radio (left panels) and gravitational wave samples (right panels). The shadings represents the region containing 68% , 95% , and all the systems. In each panel we show the lines corresponding to constant chirp masses of 1.0, 1.1, 1.2 $M_\odot$. Black dots correspond to observations.

Table 4. The logarithm of the likelihood for all models. The missing entries correspond to to the case where the likelihood is formally $-\infty$ due to the fact that we find no model pulsars in the bin containing J0737-3039B.

Comparison	1	2	3
A	−14.24	−20.31	−16.97
AF	−19.90	–	−23.31
AP	−16.52	–	−18.27
APD05	−14.21	−19.26	−16.00
APF	−21.13	–	−23.06
APT20	−15.52	−21.27	−17.65
HP	−22.28	−27.36	−24.14
SP	−15.27	−20.11	−17.26

the first one for nearly equal mass systems with two masses close to 1.4 $M_\odot$; and the second one with small mass ratio $q \sim 0.6 - 0.7$ with binaries consisting of a neutron star with gravitational mass close to the maximum mass with relatively smaller companion. The strength of the second peak depends on the value of the maximum mass of a neutron star. For the models with the higher maximal mass the sample starts to be dominated by binaries belonging to the second peak. The authors used 20 extra different models of stellar evolution, where they have varied the parameters describing various stages of stellar and binary evolutions in order to assess the robustness of the results. The binaries with a small mass ratio has so far been overlooked in relativistic calculations of the hydrodynamical inspiral or the merger phase. In that paper, the gravitational wave selected sample was compared with the volume limited sample. The volume limited sample contained only the binaries potentially detectable in gravitational waves, i.e. those younger that 10Gyr.

Up to now there was no detailed comparison of properties of neutron star binaries observed in radio and in gravitational waves. The only paper (Gondek-Rosińska et al. 2005b) that dealt with a similar problem contained a discussion of radio observability of the gravitational wave selected sample, within a single model of binary evolution with a wide initial neutron star mass spectrum. The authors assumed that the radio selected sample consists only of binaries with lifetimes (from formation till merger) longer than 100 Myrs, and there was no upper limit on the radio lifetime other that the Hubble time. They were observable as pulsars for the entire lifetime of the binary. In that paper it was shown that binary radio pulsars, which are extended systems, were only a few percent of all binary neutron stars observed in gravitational waves. The binary pulsars observed in the radio had mass ratio distribution clustered around unity. The long lived systems evolved without the possibility of significant accretion onto a neutron star while the short lived systems (with $t_{\rm grav} < 100$ Myrs) did undergo common envelope episodes with hypercritical accretion onto the neutron star. This common envelope episodes had two consequences: they tightened the orbits and led to decrease of the mass ratio of the final double neutron star system, as one of the neutron stars accreted some matter. This implied that the mass distribution of the gravitational wave selected sample of double neutron star binaries was different than the radio selected one.

Here we present a comparison of the radio selected sample of double neutron star binaries, taking into account selection effects, with the gravitational wave selected one. The radio population contains also the binaries with merger times above the Hubble time.

In Figure 5 we present the distributions of expected objects in the plane spanned by the mass ratio and the primary mass defined as the more massive component of a binary for APD05, HP and SP models. The left panels correspond to the radio selected sample while the right panels show the gravitational wave selected ones. The objects contained in the radio sample are weighted by the time they are observable as pulsar from Earth, while the objects in the gravitational wave selected sample are weighted by the volume in which they are observable. The solid lines correspond to constant values of the chirp mass in these coordinates. Observed binary neutron stars are shown as black dots. In addition on Figure 6 we show the chirp mass distributions of the binaries selected by their observability in the radio band, and by their observability in gravitational waves.

Comparing our radio selected sample with the data from Table 1 we see that the APD05 (top panel) and SP (lower panel) models are more consistent with observations than the HP (middle panel) model in which majority of binary radio pulsars are predicted to have $q < 0.8$ and one massive neutron star with $m_2 > 1.6 M_\odot$. The APD05 model, which reproduces best the observed distribution of pulsars in the $P - \dot{P}$ diagram, is consistent with most of the observed binary radio pulsars. It does also reproduce very well the chirp mass distribution of the radio observed sample. The binary neutron stars with low mass ratios and moderate masses are not predicted in this model. However, one must take into account the fact that measurements of masses of J1811-1736 and J1518+4904 carry quite large error bars. The SP model reproduces the distribution of masses and mass ratios of all observed neutron star binaries. In this model the distribution of masses is wide. It predicts existence of binaries containing massive neutron stars, however the radio selected distribution is concentrated around $q \sim 0.8 - 0.9$ and primary masses $\sim 1.35 M_\odot$.

A comparison of radio selected sample with the gravitational wave one shows visible differences for SP and HP models and negligible for the APD05 model (see also Figure 6). In the model APD05, the two samples are very similar as expected. This is due to the fact that in the binary evolution model A the range of masses of newborn neutron stars is narrow comparing to the previous calculations as well the amount of matter accreted during the common envelope episode with a helium star is negligible.

In model HP the radio sample is dominated by unequal mass binaries with $q = 0.7$, $m_2 \approx 1.7 M_\odot$. However the gravitational wave selected sample the equal mass binaries with both components of about $1.4 M_\odot$ are also dominant. Also the chirp mass distributions are very different, with radio sample leaning towards the higher chirp mass binaries. This result which is apparently counterintuitive, follows from the fact that in this model we allow for substantial accretion and consequently strong recycling of the first born pulsar. This pulsar has low magnetic field and remains radio loud for a very long time, and thus it contributes significantly to the radio sample. At the same time the binary has a large chirp mass because of the strong accretion. The gravitational wave

selected sample is dominated in model HP by the short lived systems with no significant accretion episodes, and therefore contains more systems with a low chirp mass. Additionally this model fails to reproduce the radio observed distribution of masses and mass ratios.

In the SP model the gravitational wave selected sample is shifted toward the higher chirp mass values with respect to the radio selected one. This is because of the volume effect, due to the fact that the sampling volume scales as $\propto \mathcal{M}^{5/2}$. Thus the heavier binaries are observable from much larger volume in gravitational waves. The mass ratio distribution of the gravitational wave selected sample leans toward lower values because the unequal mass binaries typically contain a low mass neutron star with a more massive companion. Thus they have a higher chirp mass than the equal mass neutron star binaries that typically contain two stars with low masses. This is similar to the comparison between the gravitational wave selected and the volume limited sample presented in Bulik et al. 2004. The comparison with radio observations reveals quite and interesting feature: the distribution of chirp mass is underestimated in this model, however the observed mass ratios are relatively well reproduced, as this model leads to a wide distribution of radio observed mass ratios.

The small differences between the gravitational wave selected and the radio selected distributions of mass ratio and chirp mass in model APD05 are mainly due to the fact that the initial masses of neutron stars come from a very narrow range and we do not allow for substantial accretion. Thus most neutron star binaries have similar masses and there is no possibility to form binaries with different chirp masses or mass ratios in this model. However, once we allow for a wide distribution of neutron star initial masses or for a significant accretion the differences between the two samples start to appear.

5 CONCLUSIONS

We have modelled the evolution of binary stars leading to formation of binary neutron star. We then follow their evolution as pulsars and discuss the properties of the binary pulsars observable in radio. We discuss several models and compare the expected distribution with observations in the P-$\dot{P}$ diagram.

First of all the analysis of the binary star evolution provides little constraints on the spontaneous magnetic field decay. This was to be expected as binary pulsars are typically observed already as old and evolved objects. At the same time we see that there must be some mechanism at work which leads to decay of the magnetic field of the first born star. This can either be the spontaneous magnetic field decay, mentioned above, or the magnetic field decay due to accretion. However we noticed that in the best fitting models the amount of accreted matter is small. This is due to two factors: in some objects the propeller effect inhibits accretion, while in other the time for the accretion is small because of the fast evolutionary timescale of the companion. Moreover, the model with large mass decay scale fits the data better than the one with small value. Thus in binary pulsars the spontaneous field decay seems to be much more important than the accretion induced decay.

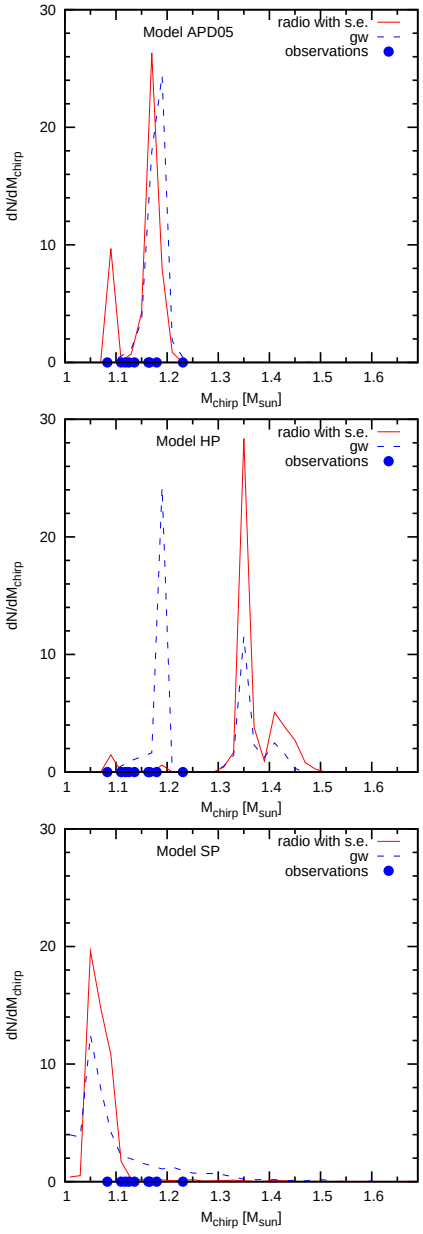

Figure 6. The distributions of chirp masses for gravitational wave selected sample and for the radio selected sample of double neutron star binaries for model APD05 (top panel), HP (middle panel) and SP (bottom panel).

The models in which we allow for substantial accretion and recycling of the neutron star lead to formation of a large number of binaries with periods below 20ms and period derivatives below $10^{-18}\mathrm{s\,s^{-1}}$. There are no observed binary pulsars in this region which means that such substantial accretion does not take place. Thus the mass accreted by the first born star must be small, or the efficiency of recycling in common envelope is very low. This efficiency can be much smaller than in the case of stable mass transfer because the mass transfer can be turbulent and we do not expect a steady transfer of angular momentum.

If the angular momentum transfer is low than we do not expect binary pulsars to have pulsation periods below $\approx$ 20ms. The binaries containing pulsars with lower period

are probably mainly neutron star - white dwarf binaries, in which the mass transfer had been stable and lasted much longer than in the progenitors of double neutron star binaries.

The orbital parameters of observed objects shows that the expected number of binary pulsars with orbital periods below 2 hours is very small. Thus, it is quite likely that the binary pulsar J0737-3039 with $P_{orb} = 2.454\,\mathrm{h}$ will remain the lowest orbital period binary pulsar for a long time. On the other hand the models hardly can explain the orbital properties of J1518+4904. Its orbital period is typical for DNS with the eccentricity of ≈ 0.8, much higher than the observed value 0.249. This eccentricity is also too large for a pulsar with a massive white dwarf companion.

Finally, we compare the properties of the radio selected and gravitational wave selected sample. We find that two different models APD05 and SP are consistent with observations. The model APD05 that best fits the distribution on the $P - \dot{P}$ diagram also reproduces well the distribution of chirp masses. In this model the binary evolution proceeds within the standard StarTrack model A, we allow for the propeller effect, partial spin-up proportional to the amount of mass accreted, and mass scale of magnetic field decay is increased to $M_d = 0.05\,M_\odot$. In this model there are very little differences between the distribution of masses in the radio and gravitational wave selected samples, and the mass ratio of binary pulsars is close to unity in both the radio and gravitational wave selected sample. However, radio observations show that there are systems with the mass ratio likely to be in the range between $0.6 - 0.9$, which do not appear in this model. The presence of such objects can be explained with the assumption that the initial mass spectrum of neutron star is wide like the one in model SP. The presence of such binaries suggests that also the unequal mass systems with the mass ratio in the range from 0.7 to unity should be included in the search for gravitational wave signals. Inclusion of a wider initial mass range on one hand widens the expected distribution of mass ratios but on the other hand decreases the agreement between the expected and observed distribution of chirp masses in the radio. This conclusions may be verified with the Square Kilometer Array observations that should reveal many more binary NS systems. The measurement of their masses along with identification of binary NS merger population by the Advanced LIGO and VIRGO will provide further insight into the properties of the population of binary neutron stars.

ACKNOWLEDGMENTS

This research was supported by the Polish Grants 1PO3D00530, N203 302835, by the European Gravitational Observatory grant EGO-DIR-102-2007, and by the FOCUS Programme of Foundation for Polish Science.

REFERENCES

Abramovici A., Althouse W. E., Drever R. W. P., Gursel Y., Kawamura S., Raab F. J., Shoemaker D., Sievers L., Spero R. E., Thorne K. S., 1992, Science, 256, 325
Arzoumanian Z., Chernoff D. F., Cordes J. M., 2002, ApJ, 568, 289
Arzoumanian Z., Cordes J. M., Wasserman I., 1999, ApJ, 520, 696
Belczynski K., Bulik T., 2002, ApJ Lett, 574, L147
Belczynski K., Bulik T., Kluźniak W. ł., 2002, ApJ Lett, 567, L63
Belczynski K., Bulik T., Rudak B., 2002, ApJ, 571, 394
Belczyński K., Kalogera V., 2001, ApJ Lett, 550, L183
Belczynski K., Kalogera V., Bulik T., 2002, ApJ, 572, 407
Belczynski K., Kalogera V., Rasio F. A., Taam R. E., Zezas A., Bulik T., Maccarone T. J., Ivanova N., 2008, ApJS, 174, 223
Benensohn J. S., Lamb D. Q., Taam R. E., 1997, ApJ, 478, 723
Bethe H. A., Brown G. E., 1998, ApJ, 506, 780
Bhattacharya D., Wijers R. A. M. J., Hartman J. W., Verbunt F., 1992, A&A, 254, 198
Blaes O., Rajagopal M., 1991, ApJ, 381, 210
Bogomazov A. I., Abubekerov M. K., Lipunov V. M., Cherepashchuk A. M., 2005, Astronomy Reports, 49, 295
Bondi H., Hoyle F., 1944, MNRAS, 104, 273
Bradaschia C., Calloni E., Cobal M., Del Fabbro R., di Virgilio A., Giazotto A., Holloway L. E., Kautzky H., Michelozzi B., Montelatici V., Passuello D., Velloso W., 1991, in Problems of Fundamental Modern Physics II VIRGO: a ground based interferometric antenna for gravitational wave detection above 10 Hz.. pp 341–356
Brandt N., Podsiadlowski P., 1995, MNRAS, 274, 461
Brown G. E., Lee C.-H., Bethe H. A., 2000, ApJ, 541, 918
Bulik T., Belczyński K., 2003, ApJ Lett, 589, L37
Bulik T., Belczyński K., Rudak B., 2004, A&A, 415, 407
Bulik T., Belczyński K., Zbijewski W., 1999, MNRAS, 309, 629
Bulik T., Gondek-Rosinska D., Belczynski K., 2004, MNRAS, 352, 1372
Buonanno A., Cook G. B., Pretorius F., 2006, ArXiv General Relativity and Quantum Cosmology e-prints
Burgay M., D'Amico N., Possenti A., Manchester R. N., Lyne A. G., Joshi B. C., McLaughlin M. A., Kramer M., Sarkissian J. M., Camilo F., Kalogera V., Kim C., Lorimer D. R., 2003, Nature, 426, 531
Cordes J. M., Kramer M., Lazio T. J. W., Stappers B. W., Backer D. C., Johnston S., 2004, New Astronomy Review, 48, 1413
Cui W., 1997, ApJ Lett, 482, L163+
de Kool M., 1990, ApJ, 358, 189
Dewi J. D. M., Podsiadlowski P., Pols O. R., 2005, MNRAS, 363, L71
Dewi J. D. M., Podsiadlowski P., Sena A., 2006, MNRAS, 368, 1742
Emmering R. T., Chevalier R. A., 1989, ApJ, 345, 931
Faucher-Giguère C.-A., Kaspi V. M., 2006, ApJ, 643, 332
Faulkner A. J., 2004, PhD thesis, Faculty of Science and Engineering, University of Manchester
Faulkner A. J., Kramer M., Lyne A. G., Manchester R. N., McLaughlin M. A., Stairs I. H., Hobbs G., Possenti A., Lorimer D. R., D'Amico N., Camilo F., Burgay M., 2005, ApJ Lett, 618, L119
Flanagan E. E., Hughes S. A., 1998, Phys. Rev., D57, 4535
Flannery B. P., van den Heuvel E. P. J., 1975, A&A, 39, 61

Fryer C. L., Woosley S. E., Hartmann D. H., 1999, ApJ, 526, 152
Gnusareva V. S., Lipunov V. M., 1985, Soviet Astronomy, 29, 645
Gondek-Rosińska D., Bejger M., Bulik T., Gourgoulhon E., Haensel P., Limousin F., Taniguchi K., Zdunik L., 2007, Advances in Space Research, 39, 271
Gondek-Rosińska D., Bulik T., Belczyński K., 2005a, Memorie della Societa Astronomica Italiana, 76, 632
Gondek-Rosińska D., Bulik T., Belczyński K., 2005b, Memorie della Societa Astronomica Italiana, 76, 513
Gonthier P. L., Ouellette M. S., Berrier J., O'Brien S., Harding A. K., 2002, ApJ, 565, 482
Gonthier P. L., Van Guilder R., Harding A. K., 2004, ApJ, 604, 775
Gunn J. E., Ostriker J. P., 1970, ApJ, 160, 979
Hartman J. W., Bhattacharya D., Wijers R., Verbunt F., 1997, A&A, 322, 477
Hobbs G., Lorimer D. R., Lyne A. G., Kramer M., 2005, MNRAS, 360, 974
Hulse R. A., Taylor J. H., 1975, ApJ Lett, 195, L51
Hurley J. R., Pols O. R., Tout C. A., 2000, Mon. Not. Roy. Astron. Soc., 315, 543
Illarionov A. F., Sunyaev R. A., 1975, Astron. Astrophys., 39, 185
Jorgensen H., Lipunov V. M., Panchenko I. E., Postnov K. A., Prokhorov M. E., 1995, ApSS, 231, 389
Kalogera V., Narayan R., Spergel D. N., Taylor J. H., 2001, ApJ, 556, 340
Kasian L., 2008, in 40 Years of Pulsars: Millisecond Pulsars, Magnetars and More Vol. 983 of American Institute of Physics Conference Series, Timing and Precession of the Young, Relativistic Binary Pulsar PSR J1906+0746. pp 485–487
Kiel P. D., Hurley J. R., Bailes M., Murray J. R., 2008, MNRAS, 388, 393
Kuiper G. P., 1935, PASP, 47, 15
Kulczycki K., Bulik T., Belczyński K., Rudak B., 2006, A&A, 459, 1001
Large M. I., 1971, in Davies R. D., Graham-Smith F., eds, The Crab Nebula Vol. 46 of IAU Symposium, The Galactic Population of Pulsars. pp 165–+
Lipunov V. M., Postnov K. A., Prokhorov M. E., Panchenko I. E., Jorgensen H. E., 1995, ApJ, 454, 593
Lorimer D. R., 2008, Living Reviews in Relativity, 11, 8
Lyne A. G., Burgay M., Kramer M., Possenti A., Manchester R. N., Camilo F., McLaughlin M. A., Lorimer D. R., D'Amico N., Joshi B. C., Reynolds J., Freire P. C. C., 2004, Science, 303, 1153
Lyne A. G., Manchester R. N., Taylor J. H., 1985, MNRAS, 213, 613
Lyutikov M., Thompson C., 2005, ApJ, 634, 1223
Manchester R. N., Hobbs G. B., Teoh A., Hobbs M., 2005, VizieR Online Data Catalog, 7245, 0
Miyamoto M., Nagai R., 1975, PASJ, 27, 533
Narayan R., Ostriker J. P., 1990, ApJ, 352, 222
Paczynski B., 1990, ApJ, 348, 485
Peters P. C., 1964, Phys. Rev., 136, B1224
Piran T., 1992, in American Institute of Physics Conference Series Vol. 272 of American Institute of Physics Conference Series, γ-ray bursts and neutron star mergers-possibly the strongest explosions in the universe. pp 1626–1633
Popov S. B., Colpi M., Treves A., Turolla R., Lipunov V. M., Prokhorov M. E., 2000, Astronomical and Astrophysical Transactions, 19, 471
Portegies Zwart S. F., Yungelson L. R., 1998, A&A, 332, 173
Rudak B., Ritter H., 1994, MNRAS, 267, 513
Scalo J. M., 1986, Fundamentals of Cosmic Physics, 11, 1
Stairs I. H., 2004, Science, 304, 547
Stollman G. M., 1987, A&A, 178, 143
Story S. A., Gonthier P. L., Harding A. K., 2007, ApJ, 671, 713
Taylor J. H., Manchester R. N., 1977, ApJ, 215, 885
Timmes F. X., Woosley S. E., Weaver T. A., 1996, ApJ, 457, 834
Vanbeveren D., De Loore C., Van Rensbergen W., 1998, AAPR, 9, 63
Weaver T. A., Woosley S. E., 1993, Phys. Rep., 227, 65
Webbink R. F., 1984, ApJ, 277, 355
Woosley S. E., 1986, in Audouze J., Chiosi C., Woosley S. E., eds, Saas-Fee Advanced Course 16: Nucleosynthesis and Chemical Evolution Nucleosynthesis and Stellar Evolution. pp 1–+
Young M. D., Manchester R. N., Johnston S., 1999, Nature, 400, 848